Mon. Not. R. Astron. Soc. **000**, 000–000 (0000) Printed 28 September 2016 (MN LATEX style file v2.2)

Galaxy Zoo: The interplay of quenching mechanisms in the group environment

R. J. Smethurst,[1] C. J. Lintott,[1] and the Galaxy Zoo team ⋆
[1] *Oxford Astrophysics, Department of Physics, University of Oxford, Denys Wilkinson Building, Keble Road, Oxford, OX1 3RH, UK*

28 September 2016

ABSTRACT
Does the environment of a galaxy directly influence the quenching timescale of a galaxy? Here we construct a sample of group and field galaxies with morphological classifications from Galaxy Zoo 2 and use Bayesian inference to determine the quenching time and exponential timescale that describes a simple SFH for a given galaxy from its photometry. We observe how the detailed morphological structures, such as bars and bulges, are affected by environment and correlate this with changes in the quenching timescales. Mass quenching is seen to be just as important for satellite galaxies as central galaxies. We find that the environment does play a direct role in galaxy quenching through a mechanism which is correlated to the halo mass of a group. It is not correlated with the relative velocity of satellite galaxies within the group, therefore mechanisms such as ram pressure stripping are not the main cause of quenching in the group environment.

Key words: galaxies – environment, galaxies – photometry, galaxies – statistics, galaxies – morphology

1 INTRODUCTION

There are many mechanisms which are proposed to cause quenching; including mergers (Daddi et al. 2010; Darg et al. 2010a; Cheung et al. 2012; Barro et al. 2013; Pontzen et al. 2016), AGN feedback (Di Matteo et al. 2005; Nandra et al. 2007), mass quenching (Peng et al. 2012), morphological quenching (Fang et al. 2013) and the environment of a galaxy (see review of mechanisms in Boselli & Gavazzi 2006, and references therein).

The galaxy environment as a cause of quenching was proposed due to the correlation of morphology (Dressler 1980; Smail et al. 1997; Poggianti et al. 1999; Postman et al. 2005; Bamford et al. 2009), SFR and the quenched galaxy fraction (Kauffmann et al. 2003; Baldry et al. 2006; Peng et al. 2012; Darvish et al. 2016) with environmental density. However, does this correlation truly imply causation? Recent evidence from simulations suggests that the environment may not be the dominant quenching mechanism in the galaxy lifecycle. Perhaps instead, the correlation of increased galaxy quenched fractions with environment is due to a superposition of the effects of mergers, interactions and both mass & morphology quenching.

⋆ This investigation has been made possible by the participation of over 350,000 users in the Galaxy Zoo project. Their contributions are acknowledged at `http://authors.galaxyzoo.org`

1.1 Mergers as a quenching mechanism

In denser environments, galaxies are more likely to encounter another galaxy in a merger or interaction scenario than when isolated in the field environment. When two galaxies merge, the influx of cold gas funnelled by the forces in the interaction often result in energetic starbursts and the fuelling of a central AGN, both of which can exhaust (and in the case of the AGN possibly expel) the gas required for star formation, effectively quenching the post-merger remnant galaxy.

1.2 Mass quenching

Mass quenching is the process by which a galaxy, independent of its environment, uses up its available gas for star formation via the Kennicutt-Schmidt law (Schmidt 1959; Kennicutt 1998) and consequently grows in mass. This is thought to be the dominant mechanism for isolated galaxies in the field. In groups and cluster environments, infall into the group can occur over long timescales during which gas reservoirs can be depleted via this mass quenching process.

1.3 Morphological quenching

Morphological quenching (or secular quenching) is the process by which the internal structure of a galaxy can impact on its SFR. This is theorised to occur in galaxies hosting

bars; the bar funnels gas to the centre of the galaxy where it is exhausted by star formation effectively quenching the galaxy. Such a process has been postulated to be caused also by bulges () and spiral () structures in galaxies.

1.4 Environmental quenching

The mechanisms under the umbrella of environmental quenching are numerous and varied. They include hydrodynamic interactions occurring between the cold inter stellar medium (ISM) of the in-falling galaxy and the hot intergalactic medium (IGM) of the group or cluster. This includes such processes as ram pressure stripping (Gunn & Gott 1972), viscous stripping (), and thermal evaporation (). Starvation () can remove the outer galaxy halo cutting off the star formation gas supply to a galaxy and preprocessing occurs when all of the above mechanisms take place in a group of galaxies which then falls into a larger cluster ().

The most likely candidate (and therefore the most studied) mechanism for the cause of the environmental density-morphology and SFR relations is ram pressure stripping (RPS). However, there has been mounting evidence that RPS may not be effective at quenching as first thought (Emerick et al. 2016; Fillingham et al. 2016).

1.5 Aims of this work

In order to isolate the case of the density-morphology and density-SFR correlations, we need to study how galaxy quenching timescales and morphology change in group and field environments with different properties. We use the group environment to study this problem, as this is a more typical environment for a galaxy then the relatively rare rich cluster environment (Carlberg 2004). To do this we construct a sample of both group and field galaxies and utilise Bayesian inference to determine the quenching time and exponential timescale to describe a simple SFH for a galaxy given its photometry. We aim to determine the following: (i) How does the environment influence the detailed morphological structures of a galaxy? (ii) Is environmental quenching occurring in the group environment?

In Section 2 we describe our data sources and inference methods and highlight our results in Section 3. We then discuss these results and how they fit into the bigger picture of quenching in Section 4. The zero points of all magnitudes are in the AB system. Where necessary, we adopt the WMAP Seven-Year Cosmology (Jarosik et al. 2011) with $(\Omega_m,\ \Omega_\Lambda,\ h) = (0.26, 0.73, 0.71)$.

2 DATA AND METHODS

2.1 Data Sources

In this investigation we use visual classifications of galaxy morphologies from the Galaxy Zoo 2[1] (GZ2) citizen science project (Willett et al. 2013), which obtains multiple independent classifications for each optical image. The full question tree for an image is shown in Figure 1 of Willett et al. The GZ2 project used 304,022 images from the Sloan Digital Sky Survey Data Release 7 (SDSS; York et al. 2000; Abazajian et al. 2009) all classified by *at least* 17 independent users, with a mean number of classifications of ~ 42.

Further to this, we required NUV photometry from the GALEX survey (Martin et al. 2005), within which $\sim 42\%$ of the GZ2 sample was observed, giving 126,316 galaxies total ($0.01 < z < 0.25$). This will be referred to as the GZ2-GALEX sample. The completeness of this sample ($-22 < M_u < -15$) is shown in Figure 2 of Smethurst et al. (2015).

Observed fluxes are corrected for galactic extinction (Oh et al. 2011) by applying the Cardelli et al. (1989) law. We also adopt k-corrections to $z = 0.0$ and obtain absolute magnitudes from the NYU-VAGC (Blanton et al. 2005; Blanton & Roweis 2007; Padmanabhan et al. 2008).

2.1.1 Group Identification

We used the Berlind et al. (2006) catalogue, which uses a friends-of-friends algorithm to identify group and cluster galaxies in the SDSS. This was cross matched to the GZ2-GALEX sample and limited to $z < 0.1$ to ensure GALEX completeness of the red sequence (see Wyder et al. 2007; Yesuf et al. 2014). Centrals were selected as the most massive galaxy in a group and all others were designated as satellites (masses were calculated using the absolute r-band magnitude and $u-r$ colour and the method of Baldry et al. 2006). The projected cluster centric radius, R, of all satellite galaxies was calculated from the projected separations of a satellite from its central (converted to kpc from a consideration of the observed redshift of the central galaxy) which was then normalised by the R_{200} of the group (the radius within which the mass overdensity is 200 times the critical density; see Finn et al. 2005), often used as a proxy for the virial radius of the group (Navarro et al. 1995). This resulted in a sample of 14,199 group galaxies with 3,468 centrals and 10,731 satellites within a projected cluster centric radius range of $0 < R/R_{200} < 25$ and $z < 0.084$.

In this work we focus on galaxies which are either quenching or quenched and are more than $\pm 1\sigma$ below the star forming 'main sequence'. This encompasses 4629 satellite and 2314 central galaxies and will be referred to as the GZ2-GROUP sample. These galaxies are highlighted in the panels of Figure 2.1 and can be seen to lie below the 'main sequence' of star formation.

2.1.2 Field sample

For all galaxies in the GZ2-GALEX sample, we calculated the smallest projected cluster centric radii, R/R_{200}, from each of the central galaxies in the Berlind et al. (2006) catalog and selected candidate field galaxies as those with (i) $R/R_{200} > 25$ and (ii) $\log \Sigma < -0.8$ (a measure of environmental density from Baldry et al. 2006). This sample of field galaxy candidates was then matched in redshift and stellar mass firstly to the central galaxies of the GZ2-GROUP sample to give 2,309 field galaxies with $z < 0.084$ which will be referred to as the GZ2-CENT-FIELD sample. In this work we focus on galaxies which are either quenching or quenched and are more than $\pm 1\sigma$ below the star forming 'main sequence'.

[1] `http://zoo2.galaxyzoo.org/`

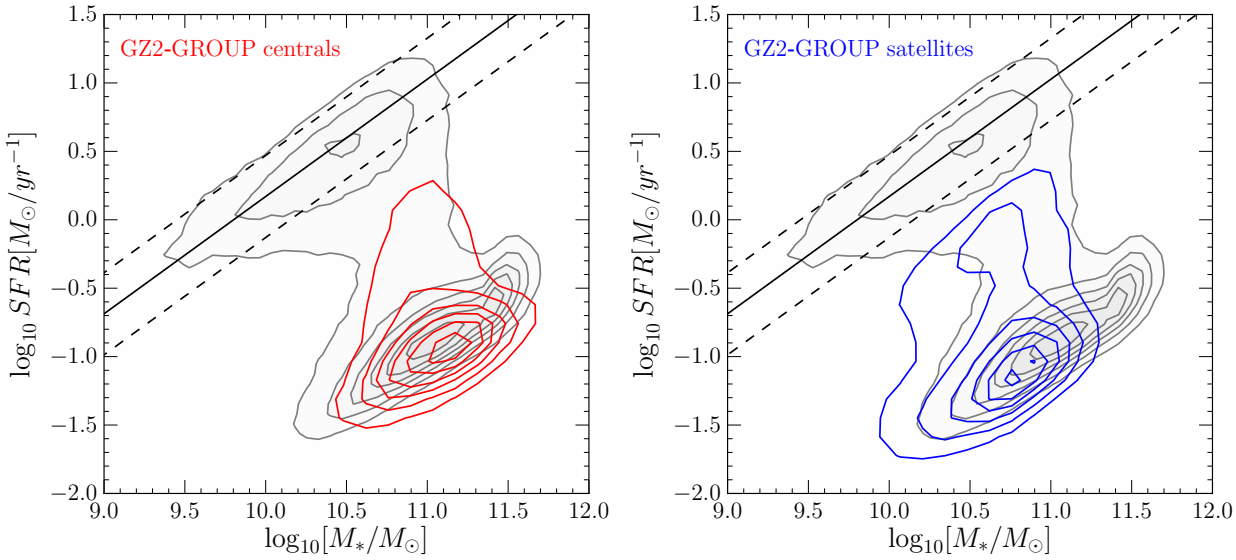

Figure 1. The SFR-stellar mass plane showing central (left; red contours) and satellite (right; blue contours) galaxies in the GZ2-GROUP sample. In both panels the entire SDSS sample from the MPA-JHU catalog is shown by the grey filled contours. The definition of the star forming "main sequence" from Peng et al. (2010) at $\overline{z} = 0.083$ (solid line, the mean redshift of the AGN-HOST sample) with $\pm 1\sigma$ (dashed lines) is shown.

This encompasses 1,596 field galaxies with $z < 0.084$ which will be referred to as the GZ2-CENT-FIELD-Q sample and used as a control sample when investigating the trends with central galaxy properties of the inferred quenching parameters.

The redshift distribution of the GZ2-CENT-FIELD-Q sample is shown in comparison to the distribution of central galaxies in the GZ-GROUP sample in Figure 2.1.2.

Secondly, the field galaxy candidates were then matched in redshift and stellar mass to the satellite galaxies of the GZ2-GROUP sample to give 6,849 field galaxies with $z < 0.084$ which will be referred to as the GZ2-SAT-FIELD. These galaxies in the GZ2-SAT-FIELD sample will be used as a control when investigating the morphological trends of satellite galaxies with environment. Note that the sample is not restricted to being $\pm 1\sigma$ below the star forming 'main sequence' in this case.

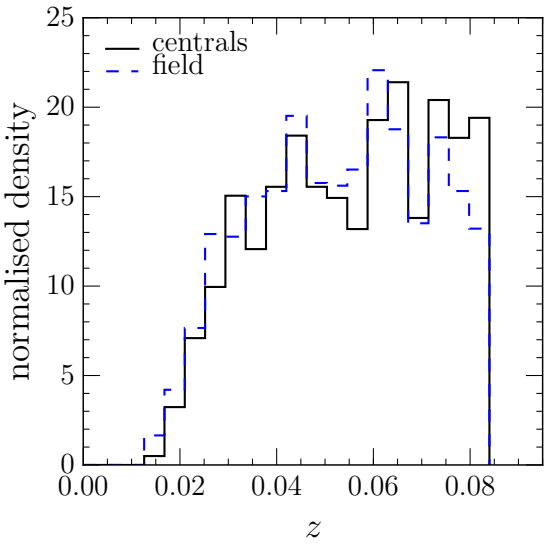

Figure 2. Redshift distributions of central galaxies in the GZ2-GROUP sample (black solid line) in comparison to the redshift and mass matched GZ2-CENT-FIELD-Q sample (blue dashed line).

2.2 Deriving quenching parameters

STARPY[2] is a PYTHON code which allows the user to derive the quenching star formation history (SFH) of a single galaxy through a Bayesian Markov Chain Monte Carlo method (Foreman-Mackey et al. 2013)[3] with the input of the observed $u-r$ and $NUV-u$ colours, a redshift, and the use of the stellar population models of Bruzual & Charlot (2003). These models are implemented using solar metallicity (varying this does not substantially affect these results; Smethurst et al. 2015) and a Chabrier IMF (Chabrier 2003) but does not model for intrinsic dust. The SFH is modelled as an exponential decline of the SFR described by two parameters $[t_q, \tau]$, where t_q is the time at the onset of quenching [Gyr] and τ is the exponential rate at which quenching occurs [Gyr]. Under the simplifying assumption that all galaxies formed at $t = 0$ Gyr with an initial burst of star formation, the SFH can be described as:

$$SFR = \begin{cases} i_{sfr}(t_q) & \text{if } t < t_q \\ i_{sfr}(t_q) \times exp\left(\frac{-(t-t_q)}{\tau}\right) & \text{if } t > t_q \end{cases} \quad (1)$$

where i_{sfr} is an initial constant star formation rate dependent on t_q (Schawinski et al. 2014; Smethurst et al. 2015).

[2] Publicly available: `http://github.com/zooniverse/starpy`
[3] `http://dan.iel.fm/emcee/`

A smaller τ value corresponds to a rapid quench, whereas a larger τ value corresponds to a slower quench. We note that a galaxy undergoing a slow quench is not necessarily quiescent by the time of observation. Similarly, despite a rapid quenching rate, star formation in a galaxy may still be ongoing at very low rates, rather than being fully quenched. This SFH model has previously been shown to appropriately characterise quenching galaxies (Weiner et al. 2006; Martin et al. 2007; Noeske et al. 2007; Schawinski et al. 2014). We note also that star forming galaxies in this regime are fit by a constant SFR with a $t_q \simeq \mathrm{Age}(z)$, (i.e. the age of the Universe at the galaxy's observed redshift) with a very low probability.

The probabilistic fitting methods to these star formation histories for an observed galaxy are described in full detail in Section 3.2 of Smethurst et al. (2015), wherein the STARPY code was used to characterise the SFHs of each galaxy in the GZ2-GALEX sample. We assume a flat prior on all the model parameters and the difference between the observed and predicted $u-r$ and $NUV-u$ colours are modelled as independent realisations of a double Gaussian likelihood function (Equation 2 in Smethurst et al. 2015). We also make the simplifying assumption that the age of each galaxy, t_{age} corresponds to the age of the Universe at its observed redshift, t_{obs}.

We note also that galaxy colours were not corrected for intrinsic dust attenuation. This is of particular consequence for disc galaxies, where attenuation increases with increasing inclination. Buat et al. (2005) found the median value of the attenuation in the GALEX NUV passband to be ~ 1 mag. Similarly Masters et al. (2010) found a total extinction from face-on to edge-on spirals of 0.7 and 0.5 mag for the SDSS u and r passbands and show spirals with $\log(a/b) > 0.7$ have signs of significant dust attenuation. However, we showed from an investigation into this problem in Section 2.2 of Smethurst et al. (2016) that internal galactic extinction does not systematically bias our results from STARPY.

The output of STARPY is probabilistic in nature and provides the posterior probability distribution across the two-parameter space for an individual galaxy the degeneracies for which can be seen in Figure 4 of Smethurst et al. (2015). Whereas in previous studies that distributions have been weight and combined to give an overall distribution representing the population of galaxies (see Smethurst et al. 2015, 2016), due to the complex nature of the group environment here we choose instead to take the 50th percentile walker position of these individual posterior probability distributions to give the most likely t_q and τ for each galaxy.

This simplifies the output from STARPYfor each galaxy from a probability distribution to two more manageable values. In this work we will look for trends in the time since quenching onset, Δt, for a given galaxy by calculating $\Delta t = t_{\mathrm{obs}} - t_q$. We will observe how this quantity changes with group properties, including halo mass (here we use the stellar mass of the group central as a proxy for halo mass), velocity dispersion, number of group members and relative velocity of a satellite galaxy.

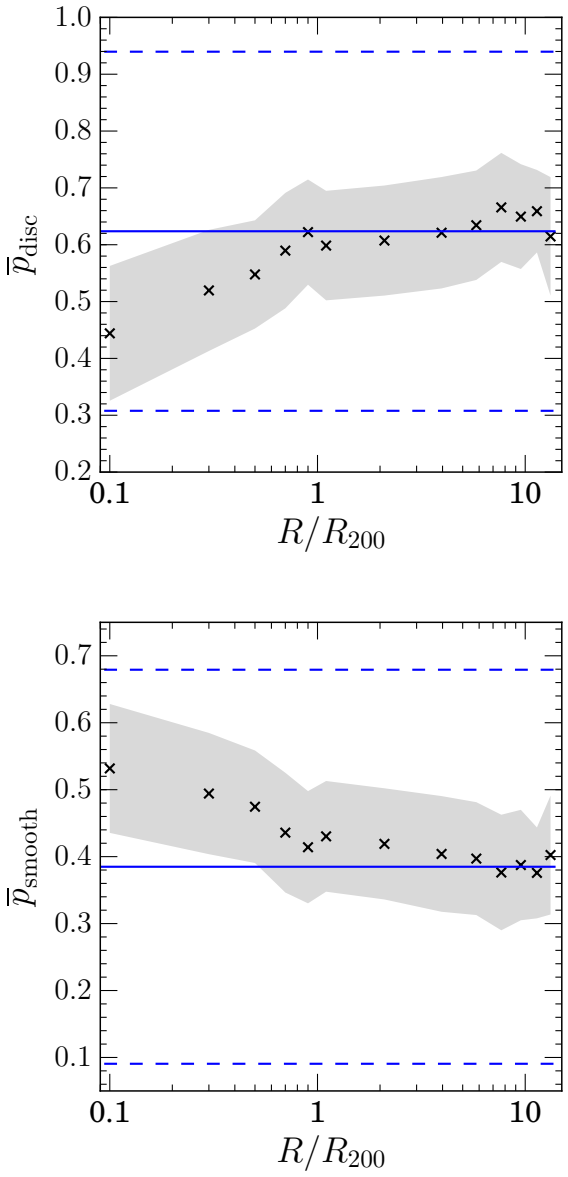

Figure 3. Mean GZ vote fraction for disc (top) and smooth (bottom) galaxies in the GZ2-GROUP sample binned in projected cluster centric radius, normalised by R_{200}, a proxy for the virial radius of a group. The shaded region shows $\pm 1\sigma$ on the mean vote fraction. The mean vote fraction of the GZ2-SAT-FIELD sample are also shown (blue solid lines) with $\pm 1\sigma$ (blue dashed lines).

3 RESULTS

3.1 Dependence of detailed morphological structure with environment

Figure 3 shows the mean disc and smooth vote fractions from galaxy zoo, binned in projected cluster centric radius (normalised by the approximate viral radius of each group, R_{200}). We can see that the mean disc (smooth) vote fraction decreases (increases) from the mean field value (blue line) under 1 virial radius in agreement with previous studies on the morphology-density relation (Dressler 1980). Along with this initial sanity check on the GZ2-GROUP sample, the ex-

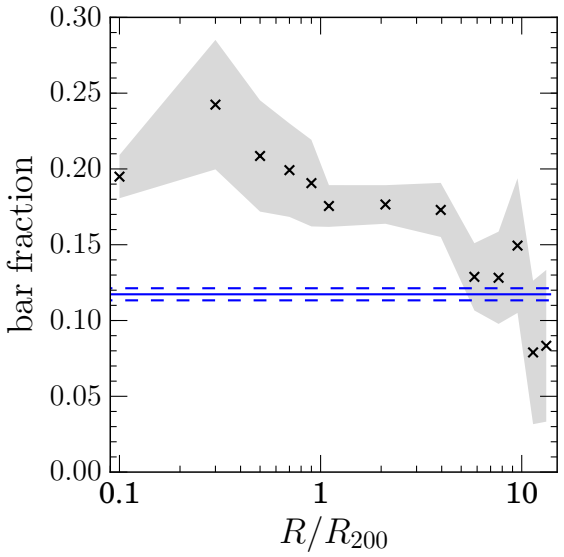

Figure 4. Bar fraction (number of barred disc galaxies over number of disc galaxies) in the GZ2-GROUP sample binned in projected cluster centric radius, normalised by R_{200}, a proxy for the virial radius of a group. The shaded region shows $\pm1\sigma$ on the bar fraction. The bar fraction of the GZ2-SAT-FIELD sample is also shown (blue solid line) with $\pm1\sigma$ (blue dashed line).

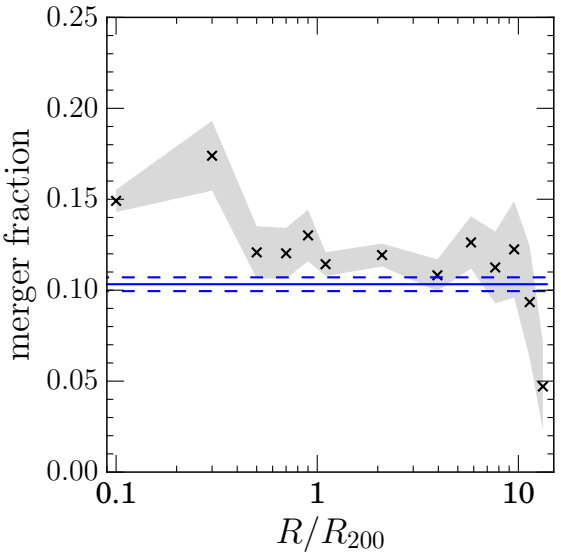

Figure 5. Merger fraction in the GZ2-GROUP sample binned in projected cluster centric radius, normalised by R_{200}, a proxy for the virial radius of a group. The shaded region shows $\pm1\sigma$ on the merger fraction. The merger fraction of the GZ2-SAT-FIELD sample is also shown (blue solid line) with $\pm1\sigma$ (blue dashed line).

tensive morphological classifications provided by GZ2 allows us to investigate how more detailed structure is affected by the group environment.

Figure 4 shows how the bar fraction (number of barred disc galaxies over the number of disc galaxies) increases towards the centre of the group population, significantly over the field fraction (blue solid line). Figure 5 shows how the merger fraction does not significantly deviate from the field fraction (blue solid line) until within $\sim$ virial radius. Similarly, the left panel of Figure 6 shows how those galaxies identified as having no or just noticeable bulges are less common in the inner regions of the cluster (left panel), whereas the fraction of galaxies with obvious or dominant bulges increases with decreasing projected distance from the centre of the cluster.

3.2 Quenching times in the group environment

With the output from STARPY we can also study the time since quenching onset ($\Delta t = t_{obs} - t_q$, see Section 2.2) binned in projected cluster centric radius, normalised by R_{200} (a proxy for virial radius) for satellite galaxies and central galaxies in the GZ2-GROUP sample, compared with galaxies in the GZ2-FIELD sample. This is shown in Figures 7 & 8 and we investigate trends in Δt by binning by various group properties:

- Stellar mass, M_*: in the top panel of Figure 7 galaxies in the GZ2-GROUP sample are now split by their stellar mass and we see a clear trend for increasing time since quenching onset with increasing stellar mass for satellite, central and field galaxies.
- Halo mass: in the middle panel of Figure 7 we use a proxy for halo mass by splitting by the GZ2-GROUP sample by the stellar mass of the corresponding central galaxy of a group, $M_{c,*}$ and find a clear trend for increasing time since quenching onset with increasing stellar mass of the group central for satellite, central and field galaxies.
- Mass ratio, $\mu_* = M_*/M_{*,c}$: the stellar mass ratio of the satellite to its central galaxy. In the bottom panel of Figure 7 we show the time since quenching of the GZ2-GROUP split into bins of $\log_{10}\mu_*$. The change in Δt with projected cluster centric radius occurs more steeply (particularly beyond $\sim$ a virial radius) for satellite galaxies with much smaller masses than their group central ($-2.0 < \log_{10}\mu_* < -1.0$, shown by the blue curve).
- Number of group members, N_{group}: the top panel of Figure 8 shows that there is no trend with time since quenching onset with increasing N_{group} for satellite galaxies. The central galaxies (shown by the square points at $\sim 0.01R/R_{200}$) however, do show a trend for increasing time since quenching with N_group.
- Relative velocity, $|\Delta v|$: in the bottom panel of Figure 8 we split the satellite galaxies of the GZ2-GROUP sample into bins of relative velocity to their central galaxies. We can see that there is no trend with time since onset of quenching with increasing relative velocity for galaxies in the group environment.
- Stellar velocity dispersion, σ_*: the bottom panel of Figure 8 shows the time since quenching of the GZ2-GROUP sample split into bins of σ_*. The stellar velocity dispersion shows the largest trend in Δt for satellite galaxies of all of the group properties studied, with galaxies with the smallest (largest) stellar velocity dispersions have quenched more (less) recently.

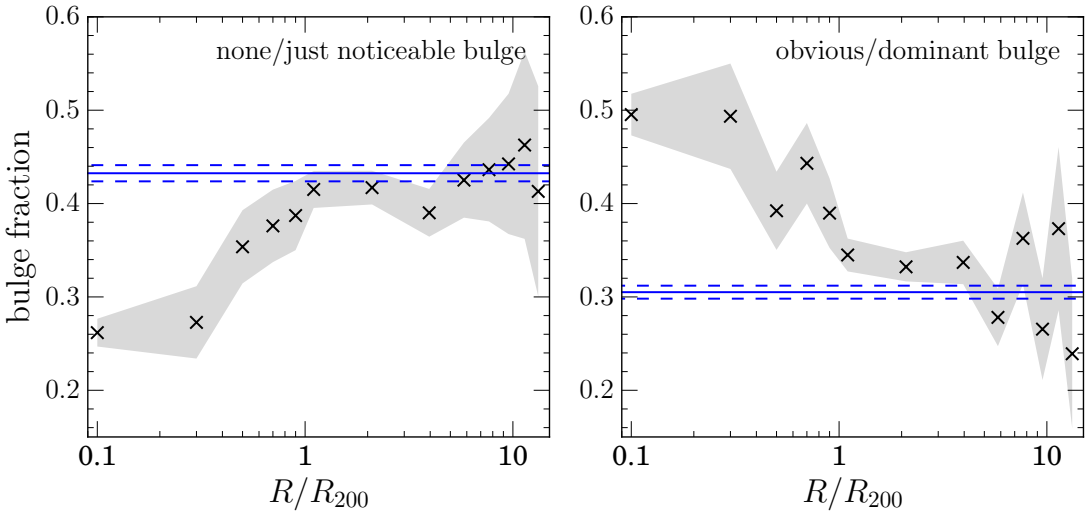

Figure 6. Fraction of galaxies with none/just noticeable bulge classifications (left) and with obvious/dominant bulge classifications (right) in the GZ2-GROUP sample binned in projected cluster centric radius, normalised by R_{200}, a proxy for the virial radius of a group. The shaded regions shows $\pm1\sigma$ on the bulge fractions. The bulge fractions of the GZ2-SAT-FIELD sample are also shown (blue solid lines) with $\pm1\sigma$ (blue dashed lines).

Across all the panels in Figures 7 & 8 we see a general trend for increasing time since quenching onset with decreasing distance from the group centre. As earlier, in Figures 3−6 significant differences from the field value arise inside $\sim$ one virial radius.

4 DISCUSSION

4.1 The role of mergers in quenching in the group environment

The merger classification in GZ2 has been shown to preferentially identify major mergers (Darg et al. 2010b). Similarly, bulge formation in disc galaxies is often associated with (minor) merger driven evolutionary histories **??**. The bulge fractions in Figure 6 vary much more significantly from the field value than the merger fraction in Figure 5. This suggests that minor mergers may be more dominant than major mergers in the group environment, particularly beyond $0.5R/R_{200}$.

If mergers are an important evolutionary mechanism for satellite galaxies as the morphological evidence in Figures 5 & 6 suggests, we would expect to see a difference in the quenching histories of satellites in groups with a higher number of galaxies, N_{group}. However, the bottom panel of Figure 7 shows that there is no trend with time since quenching onset with increasing N_{group} for the satellite galaxies. The central galaxies (shown by the square points at $\sim 0.01R/R_{200}$) however, do show a trend for increasing time since quenching with N_group. Suggesting that mergers are not the dominant quenching mechanism for satellite galaxies but are for centrals.

Velocity dispersion correlations.

4.2 The role of mass in quenching in the group environment

In the middle panel of Figure 7 the satellite galaxies of the GZ2-GROUP sample are now split by their stellar mass (calculated from the absolute r-band magnitude and $u-r$ colour by the method outlined in Baldry et al. 2006) and we do see a clear trend for increasing time since quenching onset with increasing stellar mass for both satellite and central galaxies. This is suggestive of mass quenching among the group galaxy population. This is contrary to previous work suggesting that mass quenching is only of import for central galaxies (**???**). Interestingly, the inner satellites of a given mass have quenched less recently than the centrals at the same mass range, suggesting some episode of more recent star formation may have occurred in the central galaxies but not in the inner satellites. This is once again suggestive of a merger dominated evolutionary history for central galaxies, with mergers postulated to cause a burst of star formation before then quenching the remnant galaxy (**??**Pontzen et al. 2016).

4.3 The role of morphological in quenching in the group environment

Figure 4 suggests the that the environment may play a role in triggering the disk instabilities which produce a morphological bar (**???**). This is consistent with the results that show that bars themselves may be the cause of morphological quenching through the funnelling of gas toward the central regions of galaxies () but implies that therefore implies that the quenching observed in the group population may not be due directly to an environmental quenching mechanism, but indirectly by the triggering of a bar.

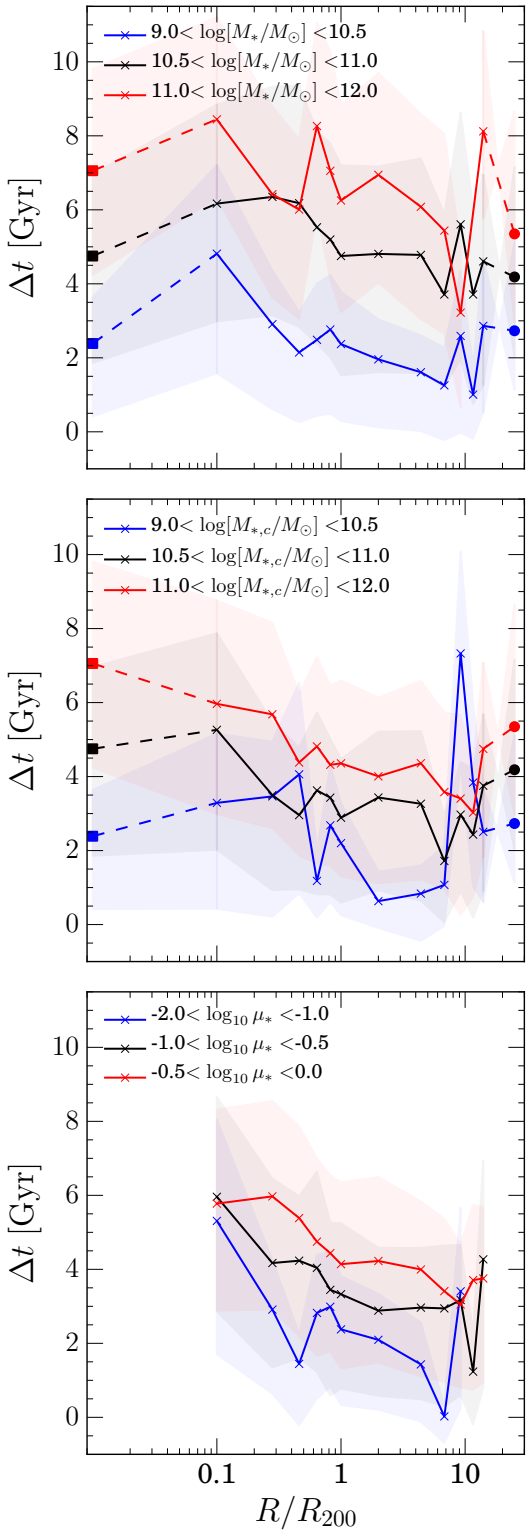

Figure 7. The time since quenching onset ($\Delta t = t_{obs} - t_q$) binned in projected cluster centric radius, normalised by R_{200}, for satellite galaxies (triangles) split by stellar mass of the corresponding central galaxy (top), stellar mass (middle) and the number of galaxies within the group (bottom). The corresponding values for central galaxies (squares) and galaxies in the GZ2-CENT-FIELD-Q sample (circles) are shown and connected by the dashed lines to aid the reader.

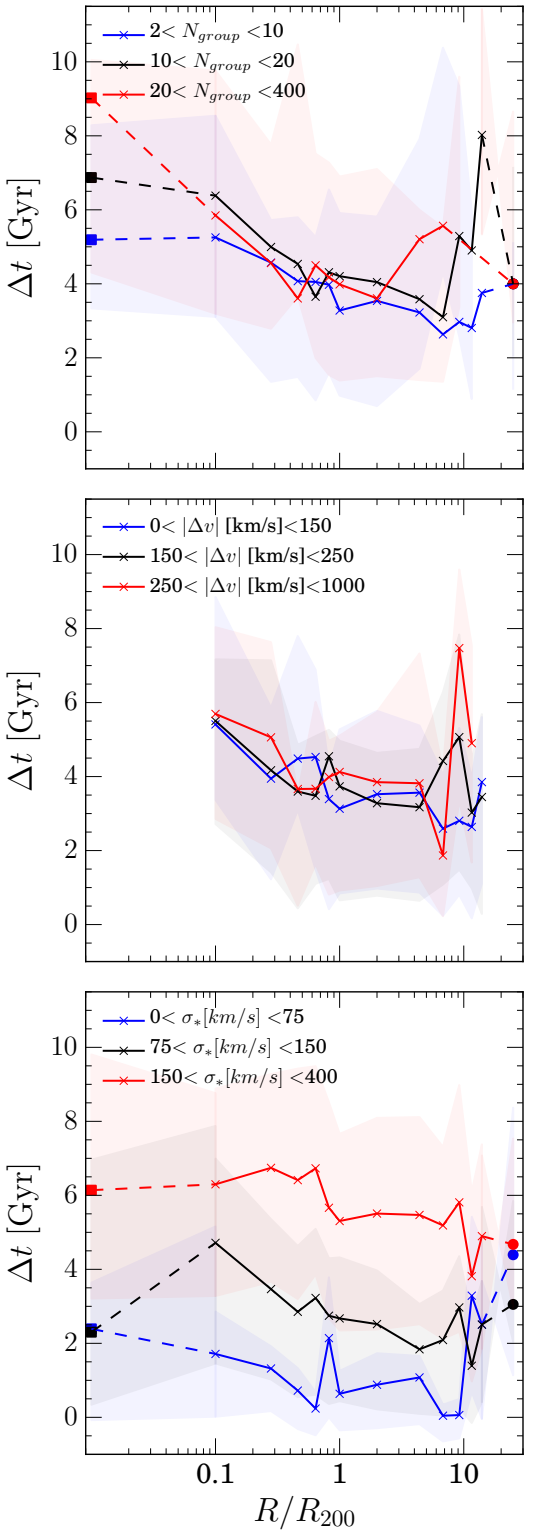

Figure 8. The time since quenching onset ($\Delta t = t_{obs} - t_q$) binned in projected cluster centric radius, normalised by R_{200}, for satellite galaxies (triangles) split by velocity dispersion (top), stellar mass ratio ($\mu_* = M_*/M_{*,c}$) (middle) and the difference in velocity from the associated central galaxy (bottom). The corresponding values for central galaxies (squares) and galaxies in the GZ2-CENT-FIELD-Q sample (circles) are shown and connected by the dashed lines to aid the reader in the top panel where appropriate.

4.4 The role of the environment in quenching

Across all panels of Figures 7-8 a trend for increasing time since quenching onset with decreasing projected cluster centric radius was present. This suggests that the environment does directly cause quenching; galaxies closer in, fell into the group earlier and as they did so they started to quench giving rise to a larger Δt.

We can also account for both the stellar mass and the halo mass of the central galaxy simultaneously by considering the stellar mass ratio of the satellite to its central galaxy, $\mu_* = M_*/M_{*,c}$, once again using the stellar mass of the central galaxy as a proxy for halo mass. In the middle panel of Figure 8 we show the time since quenching of the GZ2-GROUP sample with projected cluster centric radius split into bins of μ_*. The change in Δt with projected cluster centric radius occurs more steeply (particularly beyond $\sim$ a virial radius) for satellite galaxies with much smaller masses than their group central ($-2.0 < \log_{10}\mu_* < -1.0$, shown by the blue curve). Since the stellar mass of the central galaxy is correlated with the halo mass and therefore the potential of the system, this suggests that smaller mass galaxies in larger halos are most effected by environmental effects, therefore the dominant environmental quenching mechanism must be correlated with the group potential.

This is shown in the top panel of Figure 7 where we can once again see a clear trend for increasing time since quenching onset with increasing stellar mass of the group central for both satellite and central galaxies. More massive halos therefore have a greater impact on the star formation histories of their satellites than less massive halos. This is often though to be attributed to hotter inter galactic medium (IGM) temperatures in higher mass halos which can then impact on a galaxy through ram pressure stripping (RPS) of gas for star formation. If RPS is indeed a dominant environmental quenching mechanism we should therefore see a trend in Δt with the speed of a satellite galaxy relative to the group central. In the bottom panel of Figure 8 we split the satellite galaxies of the GZ2-GROUP sample into bins of relative velocity to their central galaxies. We can see that there is no trend with time since onset of quenching with increasing relative velocity for satellite galaxies, however the trend with decreasing projected group centric radius, seen in each panel in Figure 7 is still present. This suggests that any environmental processes causing this quenching are not corrected with satellite velocity and therefore RPS is not the dominant environmental quenching mechanism, in support of the conclusions of **?**.

This suggests that whatever environmental mechanism is at play here, it is dependant on the size of the halo, either due to the potential or temperature of the halo, but not dependant on the speed of the satellite. This suggests that ram pressure stripping is not the dominant environmental quenching mechanism at play.

We have shown that mergers are important for centrals not for satellites in the bottom panel of Figure 7. That mass quenching is important for satellites as well as centrals in the middle panel of Figure 7 and that larger halos have a stronger environmental effect on their satellites in the top panel of Figure 7.

4.5 The Big Picture

In Section 3 we have discussed how our results of the changing morphological features and quenching timescales with projected cluster centric radius in the group and field environments show evidence for both merger driven, secular and environmentally driven evolutionary histories. This suggests that not one mechanism is dominant in the group environment but that a superposition of all these effects gives rise to the observed morphology-density and morphology-SFR relations.

All these mechanisms are striving towards the same end result with no single mechanisms dominating over the other. Those mechanisms traditionally associated with the field, such as mass & morphology quenching can also occur in more dense environments, however will often eventually (after a long enough infall) be overwhelmed by those more rapid and violent mechanisms of mergers and interactions (and the triggered outflows from AGN that are associated with such mechanisms; see Smethurst et al. 2016). Similarly, environmental quenching mechanisms caused by the dense halo and IGM are at work as soon as a galaxy falls into a group or cluster, but such a process can be interrupted momentarily by an interaction or a merger as a galaxy enters the more dense environment.

Just as morphology is a spectrum from disc-dominated to spheroid-dominated systems, so too are the quenching mechanisms which cause this morphological transformation. Mergers and interactions are a spectrum of mass ratios from the micro mergers (**?**) through to major mergers, with increasing impact upon the morphology and SFR of a galaxy. Secular quenching mechanisms are a spectrum of stellar mass, with a larger impact on those galaxies with smaller masses. Environmental quenching mechanisms are a spectrum of increasing halo potential, giving rise to a stronger impact on the SFR of smaller mass galaxies in larger halos.

All of these mechanisms coalesce and will give rise to the distributions in galaxy properties we see across the Universe through their constant interplay across cosmic time.

5 CONCLUSIONS

Mass quenching is definitely prevalent for satellites and mergers are important only in the most inner regions of groups for central galaxies. The environment does play a role in quenching galaxies through a mechanism proportional to the halo mass of the group but which isn't proportional to the speed the satellite galaxy is moving at relative to its central galaxy. This suggests that ram pressure stripping is therefore not the dominant mechanism at work in environmental quenching.

Everything in cahoots.

REFERENCES

Abazajian K. N. et al., 2009, ApJS, 182, 543
Baldry I. K., Balogh M. L., Bower R. G., Glazebrook K., Nichol R. C., Bamford S. P., Budavari T., 2006, MNRAS, 373, 469
Bamford S. P. et al., 2009, MNRAS, 393, 1324
Barro G. et al., 2013, ApJ, 765, 104

Berlind A. A. et al., 2006, ApJS, 167, 1
Blanton M. R., Eisenstein D., Hogg D. W., Schlegel D. J., Brinkmann J., 2005, ApJ, 629, 143
Blanton M. R., Roweis S., 2007, AJ, 133, 734
Boselli A., Gavazzi G., 2006, PASP, 118, 517
Bruzual G., Charlot S., 2003, MNRAS, 344, 1000
Buat V. et al., 2005, ApJ, 619, L51
Cardelli J. A., Clayton G. C., Mathis J. S., 1989, ApJ, 345, 245
Carlberg R. G., 2004, Clusters of Galaxies: Probes of Cosmological Structure and Galaxy Evolution, 343
Chabrier G., 2003, PASP, 115, 763
Cheung E. et al., 2012, ApJ, 760, 131
Daddi E. et al., 2010, ApJ, 714, L118
Darg D. W. et al., 2010a, MNRAS, 401, 1552
Darg D. W. et al., 2010b, MNRAS, 401, 1043
Darvish B., Mobasher B., Sobral D., Rettura A., Scoville N., Faisst A., Capak P., 2016, ApJ, 825, 113
Di Matteo T., Springel V., Hernquist L., 2005, Nature, 433, 604
Dressler A., 1980, ApJ, 236, 351
Emerick A., Mac Low M.-M., Grcevich J., Gatto A., 2016, ApJ, 826, 148
Fang J. J., Faber S. M., Koo D. C., Dekel A., 2013, ApJ, 776, 63
Fillingham S. P., Cooper M. C., Pace A. B., Boylan-Kolchin M., Bullock J. S., Garrison-Kimmel S., Wheeler C., 2016, MNRAS
Finn R. A. et al., 2005, ApJ, 630, 206
Foreman-Mackey D., Hogg D. W., Lang D., Goodman J., 2013, PASP, 125, 306
Gómez P. L. et al., 2003, ApJ, 584, 210
Gunn J. E., Gott, III J. R., 1972, ApJ, 176, 1
Jarosik N. et al., 2011, ApJS, 192, 14
Kauffmann G. et al., 2003, MNRAS, 346, 1055
Kennicutt, Jr. R. C., 1998, ApJ, 498, 541
Martin D. C. et al., 2005, ApJ, 619, L1
Martin D. C. et al., 2007, ApJS, 173, 342
Masters K. L. et al., 2010, MNRAS, 405, 783
Nandra K. et al., 2007, ApJ, 660, L11
Navarro J. F., Frenk C. S., White S. D. M., 1995, MNRAS, 275, 56
Noeske K. G. et al., 2007, ApJ, 660, L43
Oh K., Sarzi M., Schawinski K., Yi S. K., 2011, ApJS, 195, 13
Padmanabhan N. et al., 2008, ApJ, 674, 1217
Peng C. Y., Ho L. C., Impey C. D., Rix H.-W., 2010, AJ, 139, 2097
Peng Y.-j., Lilly S. J., Renzini A., Carollo M., 2012, ApJ, 757, 4
Poggianti B. M., Smail I., Dressler A., Couch W. J., Barger A. J., Butcher H., Ellis R. S., Oemler, Jr. A., 1999, ApJ, 518, 576
Pontzen A., Tremmel M., Roth N., Peiris H. V., Saintonge A., Volonteri M., Quinn T., Governato F., 2016, ArXiv e-prints, 1607.02507
Postman M. et al., 2005, ApJ, 623, 721
Schawinski K. et al., 2014, MNRAS, 440, 889
Schmidt M., 1959, ApJ, 129, 243
Smail I., Dressler A., Couch W. J., Ellis R. S., Oemler, Jr. A., Butcher H., Sharples R. M., 1997, ApJS, 110, 213
Smethurst R. J. et al., 2016, MNRAS
Smethurst R. J. et al., 2015, MNRAS, 450, 435
Weiner B. J. et al., 2006, ApJ, 653, 1049
Willett K. W. et al., 2013, MNRAS, 435, 2835
Wyder T. K. et al., 2007, ApJS, 173, 293
Yesuf H. M., Faber S. M., Trump J. R., Koo D. C., Fang J. J., Liu F. S., Wild V., Hayward C. C., 2014, ApJ, 792, 84
York D. G. et al., 2000, AJ, 120, 1579